

# Method for determining a coupling function in coupled oscillators with application to Belousov-Zhabotinsky oscillators

J. Miyazaki\* and S. Kinoshita

Graduate School of Frontier Biosciences, Osaka University, Suita 565-0871, Japan

(Received 3 July 2006; published 27 November 2006)

A coupling function that describes the interaction between self-sustained oscillators in a phase equation is derived and applied experimentally to Belousov-Zhabotinsky (BZ) oscillators. It is demonstrated that the synchronous behavior of coupled BZ reactors is explained extremely well in terms of the coupling function thus obtained. This method does not require comprehensive knowledge of either the oscillation mechanism or the interaction among the oscillators, both of these being often difficult to elucidate in an actual system. These facts enable us to accurately analyze the weakly coupled entrainment phenomenon through the direct measurement of the coupling function.

DOI: [10.1103/PhysRevE.74.056209](https://doi.org/10.1103/PhysRevE.74.056209)

PACS number(s): 05.45.Xt, 82.40.Ck

## I. INTRODUCTION

A system of sustained oscillatory units having slightly different natural oscillation frequencies generates a collective rhythm through mutual interactions. Such systems are commonly observed and often serve as significant functional units in nature and technology [1–5]. In particular, they often play an essential role in living systems, such as neurons in the brain and cardiac myocytes in the heart. It is considerably important to study how such collective behaviors arise from a large number of oscillators.

As models of coupled oscillators, extensive investigations have been performed on coupled chemical oscillators, such as the Belousov-Zhabotinsky (BZ) reaction [6–16]. The BZ reaction is one of the most typical pattern formation processes in a nonequilibrium system and has a significant similarity with living systems. Its mechanism is well understood, and a numerical simulation can be performed based on the model. Marek and Stuchl [6] observed various types of synchronizations between two reactors separated by a plate perforated with a variable number of holes. Crowley and Epstein [7] actively controlled the mass flow between two reactors and observed three types of behaviors depending on the coupling strength: entrainments at in-phase and out-of-phase and oscillation death. Yoshimoto *et al.* [8] performed the same experiment on three coupled reactors with symmetric and asymmetric mass exchanges controlled by peristaltic pumps. They observed biperiodic, all-death, and two types of synchronized modes for the symmetric exchange with increasing coupling strength, while two additional types of synchronized modes were observed for the asymmetric exchange.

Several theoretical approaches have appeared in the literature to deal with such coupled oscillators; these are based on dynamical equations [2,3,17] and the group-theoretical approach [18,19]. In particular, the most commonly employed method is to deal directly with the differential equations describing coupled oscillators—i.e., the Oregonator model for the BZ reaction [20,21], including coupling terms on the

basis of a detailed knowledge of the reaction kinetics and coupling scheme. However, in nature, it is generally difficult to determine the differential equations governing the dynamics of a system. Further, it is necessary to determine the exact parameter values in order to correctly describe the system because even a small change in the parameter set would lead to a completely different collective behavior of the system.

A complementary and the most promising way to deal with such coupled oscillators is a phase model [2,3,17] in which the dynamical behavior of each oscillator is described solely by a single variable of phase under the assumption that the coupling strength and dispersion of natural frequencies are sufficiently small. The time evolution of the phase is generally expressed as

$$\frac{d\phi_i}{dt} = \omega_i + \sum_{j \neq i}^N \epsilon_{ij} q(\phi_i - \phi_j), \quad (1)$$

where  $\phi_i$  and  $\omega_i$  represent the phase and natural frequency of the  $i$ th oscillator, respectively,  $N$  the number of oscillators and  $\epsilon_{ij}$  the coupling strength between the  $i$ th and  $j$ th oscillators. The quantity  $q(\psi)$  is the coupling function that determines the collective behavior of the coupled oscillators. Kuramoto [17] showed the transition from disorder to a macroscopic entrained state by using a tractable form of the coupling function  $q(\psi) = \sin \psi$ . Since then, many studies using this form of  $q(\psi)$  have been reported to clarify the unique features of the transition [22–25]. As for the BZ reaction, there have been several studies in which the behavior of coupled BZ reactors was analytically treated by the phase model by assuming  $q(\psi) = \sin \psi$  [8,9].

However, it is necessary to exactly determine the shape of the coupling function in order to elucidate the synchronous behavior of the system. In particular, the BZ reaction behaves like a relaxation-type oscillator that is characterized by a different time scale during one period within a limit cycle and the form of  $q(\psi)$  is far from a simple sine function. Typical examples of such cases are oscillatory nerves and pacemaker cells in the heart, where the coupling function is expected to include higher-harmonic terms and the synchro-

\*Electronic address: [miyazaki@fbs.osaka-u.ac.jp](mailto:miyazaki@fbs.osaka-u.ac.jp)

nization feature would differ considerably from that of a sinusoidal form of coupling function [26–29].

In the present study, we will describe the behavior of coupled BZ reactors quantitatively in terms of the phase model through the direct measurement of  $q(\psi)$ . For this purpose, we will first propose a new method to determine  $q(\psi)$  experimentally by using two coupled oscillators. Subsequently, we will apply this method to two coupled BZ reactions and explain the unique synchronous behavior observed in this system by using the determined  $q(\psi)$ . According to the present method, the coupled oscillatory system can be treated without the full knowledge of either the detailed oscillation mechanism or the interaction among the oscillators. In addition,  $q(\psi)$ , which is determined by using two coupled oscillators, is generally useful for the analysis of a large number of coupled oscillators, when they are nearly identical oscillators. This paper provides a more extensive description of a previous study [30], stressing the importance of determining  $q(\psi)$  practically and discussing in detail about the potential applicability of the present method in various systems of coupled oscillators.

## II. METHOD FOR DETERMINING A COUPLING FUNCTION

First, we begin by reviewing a phase model [2,17]. Consider a self-sustained oscillator expressed by the set of  $M$ -dimensional differential equations

$$\frac{d\mathbf{x}}{dt} = \mathbf{f}(\mathbf{x}), \quad (2)$$

where  $\mathbf{x}$  is a dynamical variable characterizing an oscillator that is assumed to exhibit, in an approximate sense, a limit cycle within a phase space. In such a case, it is convenient to define the phase along its orbit in the vicinity of the limit cycle so that it grows uniformly in time and gains  $2\pi$  during each cycle such that

$$\frac{d\phi(\mathbf{x})}{dt} = \omega, \quad (3)$$

where  $\omega = 2\pi/T$  is the natural angular frequency of the oscillator [31]. Since the phase is a smooth function of the coordinates of  $\mathbf{x}$ , the time derivative of the phase can be written as

$$\frac{d\phi}{dt} = \sum_{k=1}^M (\partial\phi/\partial x_k)(dx_k/dt). \quad (4)$$

Let us now consider an ensemble of nearly identical oscillators coupled with each other with a weak coupling strength

$$\frac{d\mathbf{x}_i}{dt} = \mathbf{f}_i(\mathbf{x}_i) + \sum_{j \neq i}^N \epsilon_{ij} \mathbf{p}(\mathbf{x}_i, \mathbf{x}_j), \quad (5)$$

where  $\mathbf{x}_i$  represents a dynamical variable of the  $i$ th oscillator. The second term on the right-hand side represents the interactions between the  $i$ th and  $j$ th oscillators. The phase for each oscillator should be independently defined. The dynamics of the phases are then obtained as

$$\begin{aligned} \frac{d\phi_i(\mathbf{x}_i)}{dt} &= \nabla\phi(\mathbf{x}_i) \cdot \left[ \mathbf{f}_i(\mathbf{x}_i) + \sum_j^N \epsilon_{ij} \mathbf{p}(\mathbf{x}_i, \mathbf{x}_j) \right] \\ &= \omega_i + \sum_j^N \epsilon_{ij} \nabla\phi \cdot \mathbf{p}(\mathbf{x}_i, \mathbf{x}_j). \end{aligned} \quad (6)$$

Since  $\epsilon_{ij}$  is assumed to be sufficiently small, the deviation of  $\mathbf{x}_i$  from the limit cycle is considered to be small. This allows us to substitute  $\mathbf{x}_i$  with  $\mathbf{x}$  on the limit cycle  $\mathbf{x}_i^0(\phi_i)$  so as to obtain the following closed equations for the phase:

$$\frac{d\phi_i}{dt} = \omega_i + \sum_{j \neq i}^N \epsilon_{ij} q(\phi_i, \phi_j), \quad (7)$$

where  $q(\phi_i, \phi_j)$  is expressed as

$$q(\phi_i, \phi_j) = \nabla\phi(\mathbf{x}_i^0(\phi_i)) \cdot \mathbf{p}(\mathbf{x}_i^0(\phi_i), \mathbf{x}_j^0(\phi_j)). \quad (8)$$

Since  $q(\phi_i, \phi_j)$  is a periodic function of  $\phi_i$  and  $\phi_j$ , it can be expanded in a double Fourier series as

$$q(\phi_i, \phi_j) = \sum_{l,m} a_{l,m} e^{il\phi_i + im\phi_j}, \quad (9)$$

where  $a_{-l,-m} = a_{l,m}^*$ . The quantity  $q(\phi_i, \phi_j)$  includes both resonant and fast-oscillating terms, which are expressed explicitly as follows:

$$q(\phi_i, \phi_j) = \sum_l a_{l,-l} e^{il(\phi_i - \phi_j)} + \sum_{l, \pm n} a_{l,-l \pm n} e^{il(\phi_i - \phi_j)} e^{\pm in\phi_j}, \quad (10)$$

where the first term on the right-hand side represents the resonant term and the second the  $n$ th fast-oscillating harmonic mode. The latter will normally be time averaged under the assumption of a weak dispersion of natural oscillation frequencies. As a consequence,  $q(\phi_i, \phi_j)$  is effectively expressed as a periodic function of the phase difference  $q(\phi_i - \phi_j)$ .

According to Eq. (8), it is necessary to determine  $\nabla\phi$  and  $\mathbf{p}(\mathbf{x}_i^0, \mathbf{x}_j^0)$  in order to obtain the explicit form of  $q(\phi_i - \phi_j)$  in actual oscillator systems. In principle,  $\nabla\phi$  can be estimated by instantaneously applying a perturbation to an isolated oscillator and measuring the phase shift for each position on the limit cycle [29]. This method is possible only when the perturbation is well defined and easy to control. However, this is not always practical for actual oscillators, particularly when the oscillatory units are coupled through mass transfer; this is often the case for oscillator systems in a living system.

Here, we will propose a simple method to determine the coupling function for two given coupled oscillators. By writing the phase equations for coupled oscillators as

$$\frac{d\phi_1}{dt} = \omega_1 + \epsilon_{12} q(\phi_1 - \phi_2),$$

$$\frac{d\phi_2}{dt} = \omega_2 + \epsilon_{21} q(\phi_2 - \phi_1), \quad (11)$$

and assuming that it takes  $T_i + \Delta T_i$  during one rotation under the influence of mutual interactions, where  $\Delta T_i$  is the devia-

tion from the natural oscillation period, we obtain

$$2\pi = \oint d\phi_i = \int_0^{T_i+\Delta T_i} dt \frac{d\phi_i}{dt}. \quad (12)$$

By substituting Eq. (11) into Eq. (12) and assuming that the phase difference  $\psi \equiv \phi_i - \phi_j$  evolves slowly and changes very slightly during one rotation, we obtain the relation

$$2\pi = \int_0^{T_i+\Delta T_i} dt [\omega_i + \epsilon_{ij}q(\psi)] \approx (T_i + \Delta T_i)[\omega_i + \epsilon_{ij}q(\psi)]. \quad (13)$$

Thus, the coupling function is obtained for each  $\psi$  up to the first order of  $\Delta T_i(\psi)$  as

$$q(\psi) = -\frac{2\pi\Delta T_i(\psi)}{\epsilon_{ij}T_i^2}. \quad (14)$$

It is clear that  $q(\psi)$  can be obtainable by simple ways: (1) measuring the time interval between the marked events at which the phase is to be reset and (2) specifying the phase difference between the two oscillators. The determination of  $q(\psi)$  does not require comprehensive knowledge of either the oscillation mechanism or the interaction between the oscillators.

### III. EXPERIMENTAL PROCEDURES

The experimental setup for coupled BZ reactors is shown in Fig. 1(a); in this setup, two continuous-flow stirred-tank reactors (CSTR) were mutually connected through the mass flow. Figure 1(b) shows the schematics of the reactors. Each reactor was made of a glass bottle with a volume of 21 ml and having inlets and outlets at the top. Reactant solutions were supplied from two tanks containing the aqueous solutions of (i)  $\text{NaBrO}_3$  and (ii) malonic acid (MA) with  $\text{Ru}(\text{bipyridine})_3^{2+}$  through Teflon tubes connected to the inlet of each reactor. The concentrations of all feedstream species after mixing were identical for the two reactors and were as follows:  $[\text{BrO}^+] = 60 \text{ mM}$ ,  $[\text{MA}] = 30 \text{ mM}$ ,  $[\text{H}_2\text{SO}_4] = 0.9 \text{ M}$ , and  $[\text{Ru}(\text{bipyridine})_3^{2+}] = 0.3 \text{ mM}$ . The retention time of both the reactors was set at 0.5 h. The two reactors were mutually coupled through two tubes connected to a peristaltic pump. The flow rate was controlled to determine the coupling strength and kept identical for both the directions. The stirring was performed with a magnetically driven Teflon-coated bar rotating vigorously at the bottom of the reactor.

The two reactors were immersed in separate water baths with the temperatures maintained at  $21.0 \pm 0.1 \text{ }^\circ\text{C}$  and  $22.0 \pm 0.1 \text{ }^\circ\text{C}$ ; this led to natural oscillation periods of  $T_1 = 107 \pm 1 \text{ s}$  and  $T_2 = 99 \pm 1 \text{ s}$ , respectively. The oscillation period of the BZ reaction is known to be short at high temperatures, and the obtained periods qualitatively agree with this tendency. It is confirmed that the fluctuation in the oscillation period is mainly due to that in the temperature of the water bath. Excluding the reaction temperature, the experimental conditions for the two tanks were essentially identical. The reaction processes of both the reactors were monitored by

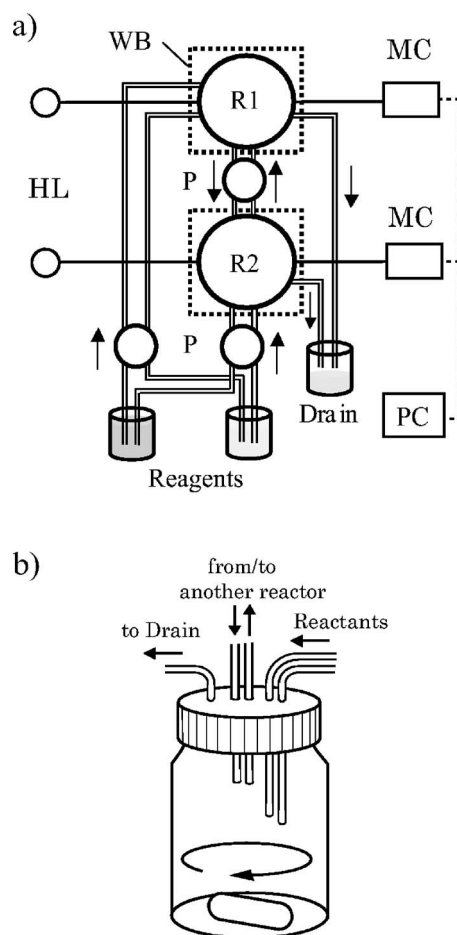


FIG. 1. Schematic view of (a) the experimental setup and (b) CSTR. HL, halogen lamp; WB, water bath; R1/2, reactor1/2; MC, monochromator; P, peristaltic pump; and PC, personal computer.

using light transmission near the absorption band of  $\text{Ru}(\text{bipyridine})_3^{2+}$  at 500 nm. A halogen lamp was employed as the light source; the light was transmitted through the reactor and detected by a fiber-coupled monochromator (Ocean Optics USB2000). The intensity of the probe light is low enough that photochemical reactions have a negligible effect on our system.

The time trace was sampled at intervals of 0.5 s and stored in a personal computer.

Here, we pay particular attention to the time-delay effect due to the mass transfer between the reactors. It is well known that a time delay causes significant effects in coupled oscillators [28,32]. This effect is prominent if the delay in flow approaches the oscillation period, owing to the difference in the temperatures between the laboratory atmosphere and water bath, as the reacting solution in a connecting tube proceeds at a different rate compared with that in the water bath, and also owing to the wall effect due to the connecting tube. In order to avoid such effects, we cut the connecting tubes sufficiently short so that the volume of connecting tubes is less than 0.25 ml; this is sufficiently small as compared with the total volume of the reactor—i.e., 21 ml. In

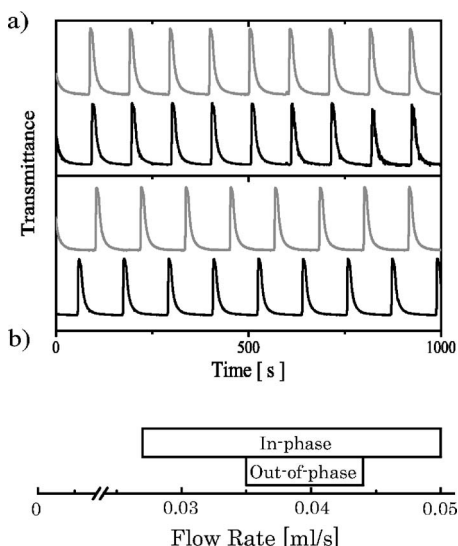


FIG. 2. (a) Time traces of in-phase (upper) and out-of-phase (lower) synchronizations. (b) Phase diagram of the synchronization modes is expressed as a function of the flow rate.

addition, we maintained the room temperature at 23 °C, closer to that of the water baths. As a result, the time delay was estimated to be negligible in the present experiment; this will be described in more detail in Sec. VII.

In the experiment and subsequent analysis, we have employed the phase of an oscillator as defined by [2]

$$\phi(t) = 2\pi \frac{t - t_k}{t_{k+1} - t_k} \quad \text{for } t_k < t < t_{k+1}, \quad (15)$$

where  $t_k$  represents the time at which the  $k$ th marked event occurs. This definition is essentially the same as that for the phase model with a zero-coupling limit and is applicable to weakly coupled systems.

Next, we examine how  $\Delta T_i$  can be measured at various  $\psi$  values. Let us suppose that the two coupled oscillators have different natural oscillation periods and that they synchronize above a critical coupling strength  $\epsilon_c$ . It is known that presynchronization occurs at a coupling strength just below  $\epsilon_c$ , where the two oscillators repeatedly assume loosely synchronized and asynchronous states [15,33,34]. In such a case,  $\psi$  evolves over  $2\pi$ ; therefore,  $\Delta T_i(\psi)$  is measurable at any value of  $\psi$ . On the other hand, when the coupling strength is above  $\epsilon_c$ , the two oscillators are normally synchronized and the value of  $\psi$  is eventually locked at a specific value of  $\psi_{sync}$ . However, if either oscillator is instantaneously perturbed or the coupling is transiently prevented,  $\psi$  will deviate from  $\psi_{sync}$ . Subsequently,  $\psi$  begins to recover to  $\psi_{sync}$  slowly as compared with the oscillation period, thereby providing an opportunity to measure  $\Delta T_i(\psi)$ . Thus, in principle,  $q(\psi)$  can be determined in the presence of coupling, irrespective of whether the coupling strength is below or above  $\epsilon_c$ .

#### IV. EXPERIMENTAL RESULTS

Figure 2(a) shows typical time traces for the two synchronizations. In our system, both the in-phase and out-of-phase

TABLE I. Oscillation periods of the in-phase and out-of-phase synchronizations for various flow rates.

	$\rho$ [ml/s]	$T_{in/out}$ [s]
In-phase	0.029	102
	0.041	102
Out-of-phase	0.035	113
	0.039	115
	0.041	117

synchronized modes are observed by increasing the flow rate  $\rho$  that is proportional to the coupling strength. It is found that only the in-phase synchronization is observed above a flow rate of  $\rho=0.027$  ml/s, while for the flow rates between 0.035 ml/s and 0.044 ml/s, both out-of-phase and in-phase synchronizations are found to be present [shown in Fig. 2(b)]. The switching between the two synchronization modes is realized by momentarily stopping the mass flow for several minutes to allow the reactors to proceed independently and then resuming the flow.

The oscillation periods of the in-phase synchronization  $T_{in}$  and out-of-phase synchronization  $T_{out}$  are listed in Table I for several flow rates. It is found that  $T_1 < T_{in} < T_2$  while  $T_{out} > T_1, T_2$ . The oscillation period of the out-of-phase synchronization  $T_{out}$  tends to become longer as the flow rate is increased, while  $T_{in}$  is rather insensitive to the flow rate. Phase slips, transitions between the two synchronous states caused by a fluctuation force, are often observed near the boundary between these oscillation states; this makes it difficult to determine the boundary definitely.

Figure 3 shows the time evolution of the phase difference  $\psi$  between the two reactors  $\psi = \phi_1 - \phi_2$ , calculated according to Eq. (15) for three different coupling strengths. In this figure, we obtain  $\psi$  at each firing event in reactor 1 and plot  $\psi$  in such a manner that it distributes within  $2\pi$ . When the two reactors oscillate independently—i.e.,  $\rho=0$ — $\psi$  is found to change constantly with time [Fig. 3(a)]. Figure 3(b) shows the time evolution of the phase difference near the in-phase synchronization at  $\rho=0.023$  ml/s; we can clearly see the presynchronization phenomenon from the presence of a periodic undulation. It appears that the two reactors tend to be loosely synchronized at the phase differences of two positions, slightly below  $2\pi$  and  $\pi$ , around which in-phase and out-of-phase synchronizations will occur at higher flow rates. Once an in-phase or out-of-phase synchronization takes place,  $\psi$  remains almost constant, as shown in Figs. 3(c) and 3(d). Hereafter, the phase differences at which the in-phase and out-of-phase synchronizations occur are specified as  $\psi_{in}$  and  $\psi_{out}$ , respectively.

#### V. ANALYSIS

In the following discussion, we will analyze the above results in terms of the phase model. For this purpose, we derive  $q(\psi)$  according to the methods described above for two typical cases: i.e., (i) presynchronization region and (ii) synchronization region. The coupling strengths  $\epsilon_{12}$  and  $\epsilon_{21}$



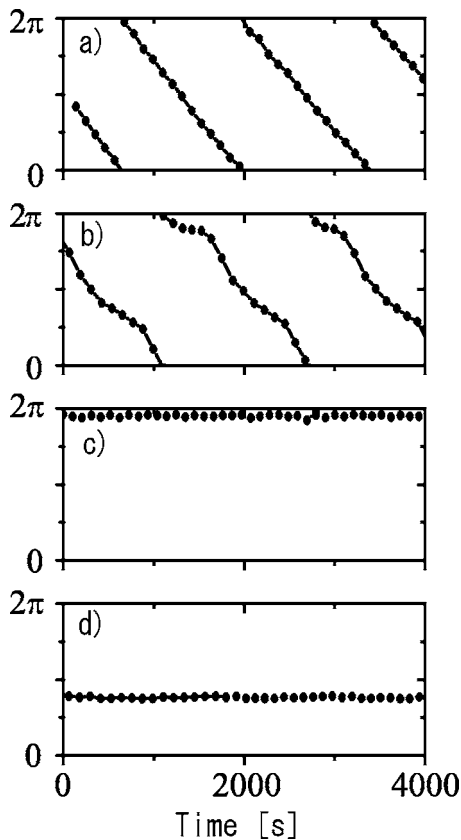


FIG. 3. Time evolution of the phase difference  $\psi$  at (a) zero coupling strength, (b)  $\rho=0.023$  ml/s, and (c),(d)  $\rho=0.037$  ml/s. (c) and (d) correspond to the in-phase and out-of-phase synchronizations, respectively.

are assumed to be equal to each other in our system and are expressed as  $\epsilon \equiv \rho/V$ , where  $V$  is the volume of the reactor.

As shown in Figs. 4(a)–4(c),  $q(\psi)$  is successfully determined in the presynchronization region. In particular,  $q(\psi)$  is most accurately determined at the coupling strength just below the synchronization threshold as seen in Fig. 4(c). This is because  $\Delta T$  due to the coupling effect becomes large as compared with that caused by the temperature fluctuation and the phase difference tends to evolve slowly.

In the synchronization region, the mass flow is transiently stopped so that each reactor oscillates at its own frequency and  $\psi$  deviates from  $\psi_{in/out}$ ; this enables the measurement of  $q(\psi)$  at various values of  $\psi$ . Figure 4(d) shows the result in which the two reactors are in the state of in-phase synchronization. The mass flow is stopped during the first or second cycle so that  $\psi$  begins to deviate from  $\psi_{in}$ , which is shown as a gray band in the figure. After resuming the flow,  $\psi$  changes considerably and approaches  $\psi_{in}$  again. If the deviation of  $\psi$  from  $\psi_{in}$  is sufficiently small,  $\psi$  tends to return to the original point. Horizontal bars for each point show the evolution of  $\psi$  during one oscillation. At a high flow rate, the time evolution of  $\psi$  becomes so large that it is difficult to choose the values of  $\psi$ .

It is clear that  $q(\psi)$ 's obtained for a suitable range of the flow rate agree well with each other; this shows the validity of the present method. Note that almost identical  $q(\psi)$ 's are

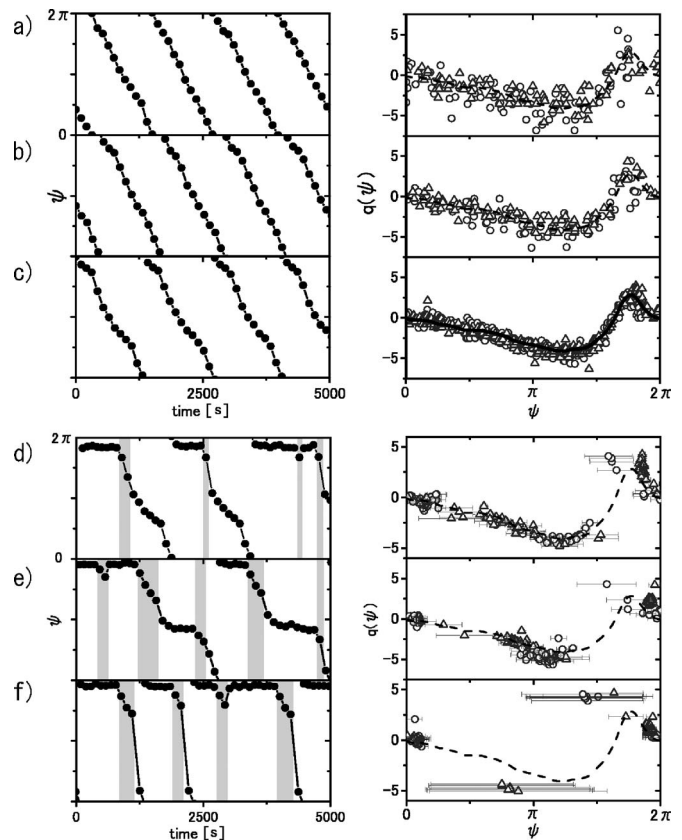


FIG. 4. Time evolution of the phase differences (left part) and coupling functions (right part) determined in the presynchronization [(a), (b), and (c)] and synchronization region [(d), (e), and (f)]. The flow rates  $\rho$  are (a)  $\rho=0.011$  ml/s, (b)  $\rho=0.0159$  ml/s, (c)  $\rho=0.022$  ml/s, (d)  $\rho=0.031$  ml/s, (e)  $\rho=0.042$  ml/s, and (f)  $\rho=0.063$  ml/s. Gray bands in the lower left represent the time, during which the mass flow was ceased. In the right part, points obtained from reactors 1 and 2 are plotted with open circles and triangles, respectively. A solid line at the flow rate of (c)  $\rho=0.022$  ml/s is obtained by a curve fit using a function  $\sum_{l=0}^{10} a_l \sin(l\psi) + b_l \cos(l\psi)$  with the fitting parameters of  $a_l$  and  $b_l$ . Dashed lines in (a), (b), and (d)–(f) are the same as the solid line, which shows the agreement among the data.

obtained for reactors 1 and 2. It is obvious that the form of  $q(\psi)$  is extremely different from that of a sinusoidal function: they are characterized by a curve that gradually decreases in the region of small values of  $\psi$  while abruptly increasing at larger values of  $\psi$ . The minimum and maximum of the curve occur around  $5/4\pi$  and  $7/4\pi$ , respectively.

Here, we describe the analysis of the experimental results by using the obtained  $q(\psi)$ . The time evolution of  $\psi$  is derived from Eq. (11) as

$$\frac{d\psi}{dt} = -\Delta\omega + \epsilon Q(\psi), \quad (16)$$

where  $Q(\psi) \equiv q(\psi) - q(-\psi)$  and  $\Delta\omega \equiv \omega_2 - \omega_1$ . Figure 5 shows  $Q(\psi)$ , which is estimated from  $q(\psi)$  in Fig. 4(c). We can then easily predict the result of changing the coupling strength  $\epsilon$ . For this purpose, we plot  $Q(\psi)$  and  $\Delta\omega/\epsilon$  for two

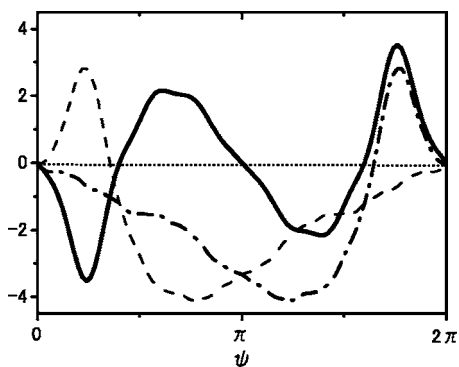


FIG. 5.  $Q(\psi)$  estimated from  $q(\psi)$  in Fig. 4(c) is shown as a solid line.  $q(\psi)$  and  $q(-\psi)$  are expressed as dot-dashed and dashed lines, respectively.

typical values of  $\epsilon$ , as shown in Fig. 6. With increasing coupling strength, a pair of stationary solutions of Eq. (16) are obtained as intersection points of  $Q(\psi)$  and  $\Delta\omega/\epsilon$ . Since the stability of the entrainment requires  $dQ(\psi)/d\psi < 0$ , only one of the two solutions can actually be realized. The phase difference of the stable solution designated as  $\psi_{in}$  asymptotically approaches  $2\pi$  with increasing  $\epsilon$ . Thus, the in-phase synchronization is realized. Since the signs of  $q(\psi_{in})$  and  $q(-\psi_{in})$  are positive and negative, respectively, the oscillation period in the in-phase synchronization mode is intermediate between the two natural oscillation periods.

At high values of  $\epsilon$ , a new stable solution appears slightly below  $\pi$  in addition to that of the in-phase synchronization. It is apparent that this stable solution will approach  $\pi$ , as  $\epsilon$  is increased. This corresponds to the out-of-phase synchronization at the phase difference designated as  $\psi_{out}$ . Thus, bistability between the out-of-phase and in-phase synchronizations can be reproduced. In the out-of-phase synchronization, the signs of  $q(\psi_{out})$  and  $q(-\psi_{out})$  are negative, and therefore the two oscillators synchronize at a longer period as compared to their natural frequencies.

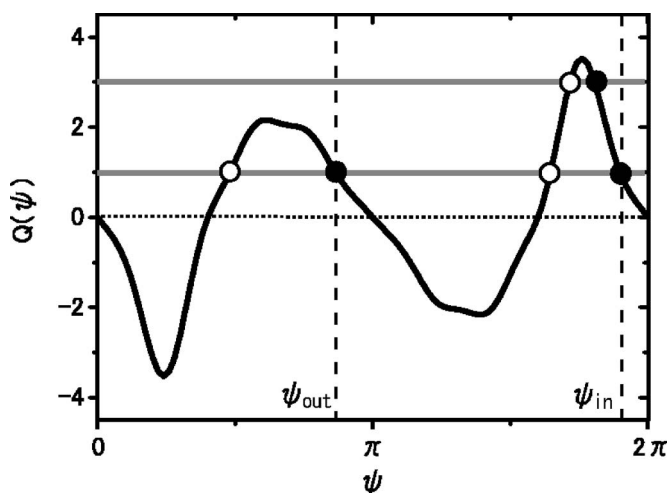


FIG. 6. Stable and unstable solutions of Eq. (16) are shown as solid and open circles, respectively, at two values of  $\Delta\omega/\epsilon$ , where the sign of  $\Delta\omega$  is positive. The stable solutions at the phase differences designated as  $\psi_{out}$  and  $\psi_{in}$  correspond to those of the out-of-phase synchronization and in-phase synchronization.

One can evaluate the critical flow rate  $\rho_c$  above which synchronization occurs by evaluating the extremal value of  $Q(\psi)$ . According to Eq. (16),  $\rho_c$  is given as  $\rho_c = \Delta\omega V / Q_{ex}$ , where  $Q_{ex}$  is the extremal value of  $Q(\psi)$ . The values of  $Q_{ex}$  that correspond to the in-phase and out-of-phase synchronizations are estimated to be 3.6 and 2.3. The corresponding values of  $\rho_c$  are estimated to be approximately 0.03 ml/s and 0.04 ml/s; these roughly agree with the actual values of 0.027 ml/s and 0.035 ml/s, respectively.

At considerably high values of  $\epsilon$ , it is natural to expect that only the in-phase synchronization should be realized as the concentrations in the two reactors approach homogeneity. However, the analysis using Eq. (16) always shows the coexistence of two stable synchronizations. In this case, the fast-oscillating terms that are neglected in Eq. (11) become crucial. A detailed discussion on this point will appear in Sec. VII.

### VI. NUMERICAL SIMULATION

In the past, controversial experimental results were frequently reported [7,8], in which an out-of-phase synchronization was first observed with increasing coupling strength followed by an in-phase synchronization. These results seem to be different from our experimental results, where an in-phase synchronization is first observed with increasing coupling strength. In these experiments, different sets of reactants and differing compositions of the BZ reaction were employed. For example, acetylacetone was used in Ref. [7] as a substitute for malonic acid and  $Ce^{3+}$  was used in Ref. [7,8] as a catalyst. Other conditions such as the dissolved oxygen, temperature, nature of the wall of the reactor, and stirring characteristics may also cause differences in experimental condition [35–39].

It is natural to suppose that  $q(\psi)$  somehow depends on the experimental condition that then results in different behaviors with changing coupling strengths. In the following paragraphs, we will examine how these experimental conditions affect the functional form of  $q(\psi)$  and alter the apparent synchronization phenomena by changing the coupling strength. To this end, it is helpful to perform a numerical simulation using a basic chemical model of BZ reaction called the Oregonator model [20,21]; this has been successfully used in describing a wide range of dynamical behaviors in BZ reactions. This model enables us to investigate the form of the coupling function for several parameter sets that characterize the reaction kinetics.

A three-variable version of the Oregonator model for reactor 1 that is coupled to reactor 2 through mass exchange is expressed by the following set of equations:

$$\frac{dx_1}{d\tau} = \delta^{-1}[x_1(1-x_1) - y_1(x_1 - q)] + \frac{c\rho_1}{V_1}(x_2 - x_1),$$

$$\frac{dy_1}{d\tau} = \delta^{-1}(-qy_1 - x_1y_1 + fz_1) + \frac{c\rho_1}{V_1}(y_2 - y_1),$$

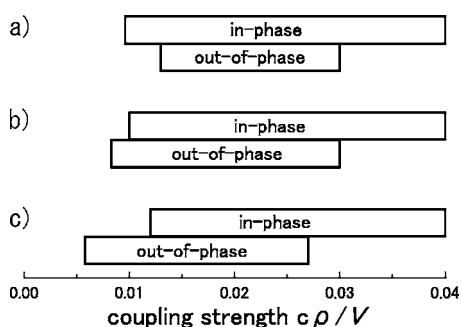


FIG. 7. Phase diagram of the synchronization modes at several values of  $f$ : (a)  $f=1.0$ , (b)  $f=1.25$ , and (c)  $f=1.5$ .

$$\frac{dz_1}{d\tau} = x_1 - z_1 + \frac{c\rho_1}{V_1}(z_2 - z_1), \quad (17)$$

with dimensionless variables and parameters  $x = [2k_4/(k_3A)]X$ ,  $y = [k_4k_5B/(k_3A)^2]Y$ ,  $z = [k_2/(k_3A)]Z$ ,  $\delta = k_5B/(k_3A)$ ,  $\delta' = 2k_4k_5B/(k_2k_3A)$ ,  $q = 2k_1k_4/(k_2k_3)$ , and  $\tau = k_5Bt$ ; here,  $A = [\text{BrO}_3^-]$ ,  $B = [\text{bromomalonic acid}] + [\text{malonic acid}]$ ,  $X = [\text{HBrO}_2]$ ,  $Y = [\text{Br}^-]$ , and  $Z = [\text{Ru}(\text{bipyridine})_3^{2+}]$ . The parameter  $k_j$  ( $j=1-5$ ) is a rate constant in the Oregonator model, and  $f$  is a stoichiometric parameter that reflects the number of  $\text{Br}^-$  ions generated through complicated organic oxidation reactions. The bromomalonic and malonic radicals play an important role in organic reactions. It is pointed out that an effective value of  $f$  may depend on several factors, such as dissolved oxygen [36]. Thus,  $f$  is often treated as an empirical parameter and typically takes a value between 0.5 and 2 [37,40]. The quantities  $\rho_i$  and  $V_i$  represent the flow rate and volume of reactor  $i$  ( $i=1,2$ ), respectively. The coupling strength is expressed as the ratio of  $\rho_i$  and  $V_i$ , which is multiplied by a scaling parameter  $c=1/(k_5B)$ . The equations for reactor 2 are given in an equivalent way. The feedstream species are not explicitly considered; the concentrations of all the input species are set as constant parameters.

In the present study, we have made a model calculation using Eq. (17) under the oscillatory condition for several values of  $f$  with varying  $c\rho/V$  while the following parameters are fixed:  $q=0.002$ ,  $\delta^{-1}=8$ , and  $\delta'^{-1}=720$ . In order to attain different natural oscillation periods for the system of two reactors, the time scale for reactor 2 is rescaled as  $0.96k_5Bt$ . Numerical integration is performed using the fourth-order Runge-Kutta method.

The calculated result shows that in-phase and out-of-phase synchronizations are present depending on the coupling strength  $c\rho/V$ , with the phase difference of the respective modes slightly below  $2\pi$  and  $\pi$ . It is also found that the oscillation period of the out-of-phase mode becomes longer than the natural periods of the reactors, while that of the in-phase mode is intermediate between them. These trends completely agree with our experiments and have been commonly observed in numerical simulations regardless of the parameter values.

It is found that the region of the synchronization modes strongly depends on  $f$ . The phase diagram of the synchroni-

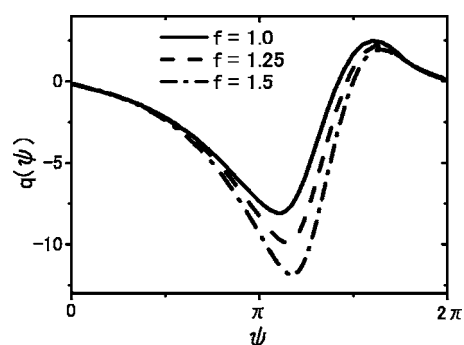


FIG. 8. Coupling functions at several values of  $f$ : solid line,  $f=1.0$ ; dashed line,  $f=1.25$ ; and dot-dashed line,  $f=1.5$ .

zation modes as a function of  $c\rho/V$  is shown in Fig. 7 for  $f=1.0, 1.25$ , and  $1.5$ . When  $f=1.0$ , the in-phase synchronization is first observed as  $c\rho/V$  is increased, while the out-of-phase synchronization appears between  $c\rho/V=0.013$  and  $0.03$ ; this trend is in good agreement with our experimental results. On the other hand, the region of the out-of-phase mode expands with increasing  $f$ , while that of the in-phase mode diminishes. Thus, the out-of-phase mode is first observed as  $c\rho/V$  is increased, while the in-phase mode appears at a higher region of  $c\rho/V$ , which appears to qualitatively agree with the results in Refs. [7,8].

In order to analyze the above result, we plot  $q(\psi)$  obtained from the numerical simulation in Fig. 8. The coupling functions  $q(\psi)$  can be characterized by a curve that gradually decreases at first and then sharply increases; these functional forms are essentially the same as those obtained from the experiments. We have found that this characteristic form holds for a wide range of parameter sets. On the other hand, their extremal values are dependent on the parameter sets, although their positions change only slightly. In particular, it is found that the negative value around  $5/4\pi$  considerably changes with increasing  $f$ .

Figure 9 shows the relation  $Q(\psi) \equiv q(\psi) - q(-\psi)$ . According to the foregoing analysis, the positive humps slightly below  $\pi$  and  $2\pi$  correspond to the solutions of the out-of-phase and in-phase synchronizations, respectively, and their absolute values determine the region of the synchronization modes when the coupling strength is changed. It is evident that the extremal value for the out-of-phase mode is larger

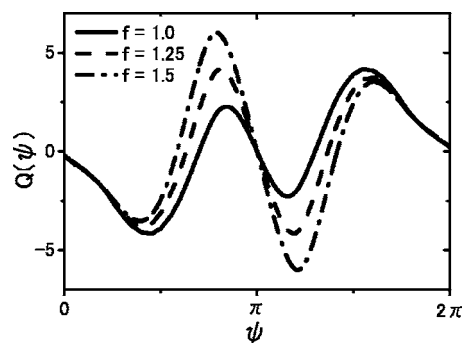


FIG. 9.  $Q(\psi)$ 's at several values of  $f$ . These are drawn by using  $q(\psi)$ 's in Fig. 8. Solid line,  $f=1.0$ ; dashed line,  $f=1.25$ ; and dot-dashed line,  $f=1.5$ .

than that for the in-phase mode at large values of  $f$ ; this relation reverses for small values of  $f$ . These results explain the phase diagrams in Fig. 7.

From the results of numerical simulation, we have found that the stable regions of the two synchronous modes depend strongly on the parameter sets of the Oregonator model; this dependence essentially originates from the change in the actual functional form of  $q(\psi)$ , although its essential shape remains unchanged. Thus, even when the behavior of coupled oscillators is simulated by using the fundamental equations, it is absolutely necessary to employ the correct parameter sets to reproduce an accurate coupling function. However, it is generally difficult to specify the exact value of the parameter sets in the Oregonator model because the BZ reaction involves complicated reaction processes, which are contracted in the course of the derivation of the Oregonator model. Furthermore, when  $\text{Ru}(\text{bipyridine})_3^{2+}$  is used as the catalyst, the Oregonator model must be modified considering the different redox potentials between  $\text{Ce}^{3+}/\text{Ce}^{4+}$  and  $\text{Ru}(\text{bipyridine})_3^{2+}/\text{Ru}(\text{bipyridine})_3^{3+}$  [40]. These complexities in the modeling of the BZ reaction lead to difficulties in elucidating the collective behavior of actual systems on the basis of a fundamental mechanism.

## VII. DISCUSSION

From the experimental study and computer simulation, we have shown that the synchronous behavior of two coupled BZ oscillators is explained well in terms of a phase model through the direct measurement of a coupling function  $q(\psi)$ . In order to obtain the relation, we only postulate the weak coupling and narrow distribution of the natural frequencies. The coupling function thus obtained differs considerably from a sinusoidal function that has often been employed in theoretical studies. It is thus important to obtain  $q(\psi)$  directly from the experiment. Our method to obtain  $q(\psi)$  is extremely simple because only marked times are recorded during the oscillatory events in the presynchronization stage or after the synchronization is temporarily perturbed. It is experimentally shown that  $q(\psi)$  obtained in the presynchronization stage gives a more favorable result. It is important to note that the present method does not require comprehensive knowledge of either the oscillation, such as the detailed mechanism of the reaction processes, or the interaction among the oscillators, both of these being often difficult to elucidate in actual systems. In addition, the coupling function can be obtained without tracing complete sets of the state vector. Thus, the present method has an enhanced capability for applications in actual coupling phenomena in nonequilibrium systems. Before closing, we will discuss a few points that are important to extend further the applicability of this method.

The first point concerns synchronization at a high coupling strength. It is natural that only the in-phase synchronization should be realized at a high coupling strength because the concentrations of the two reactors approach homogeneity. Nevertheless, the present analysis apparently shows that both in-phase and out-of-phase synchronizations can exist even at high coupling strengths.

Although it is not known to what extent a phase model is valid as a coupling strength is increased, this may be explained within the limit of the present model by considering the fast-oscillating terms in  $q(\phi_1, \phi_2)$ , which have been eliminated in Eq. (11). Note the second term in Eq. (10), which is the deviations of  $O(\epsilon)$  [2]. Then,  $Q(\psi)$  in Eq. (16) is replaced by

$$Q(\psi) + \sum_{l,n} 2ia_{l,-l\pm n} \sin[(l \mp n/2)\psi] e^{\pm in\psi/2} e^{\pm in\phi_2}, \quad (18)$$

where the term  $\sin[(l \mp n/2)\psi]$  on the right-hand side gives a nonzero value when  $\psi = \pi$  for odd  $n$ , while it gives zero regardless of  $l$  and  $n$  when  $\psi = 2\pi$ . In our experiment,  $\psi_{in}$  and  $\psi_{out}$  are approximately  $2\pi$  and  $\pi$ , respectively. Thus, the fast modes have an effect only in the out-of-phase synchronization, while they are negligible in the in-phase synchronization. As a result, the out-of-phase synchronization becomes unstable at high  $\epsilon$  possibly due to the influence of the fluctuating force. This gives a qualitative explanation for strong coupling. However, further investigation is required to quantitatively evaluate the critical coupling strength at which the out-of-phase synchronization becomes unstable, as well as to examine the validity of the phase description.

The second point is related to the effect of the time delay on the present synchronization experiment. The time delay is caused owing to the finite volume of mass transfer between the two reactors. In the present study, the oscillation period is set to be approximately 100 s and the synchronization is observed above the flow rate of 0.027 ml/s, which corresponds to a flow delay of 9.3 s. Thus, the time delay is considerably smaller than the oscillation period and is eventually negligible in the present case. In fact, the above estimation can be examined directly by comparing the  $q(\psi)$ 's obtained for several flow rates. If the time delay causes a significant effect, one expects that  $q(\psi)$  should be shifted by  $\omega\tau_d$  and result in  $q(\psi + \omega\tau_d)$  [28], where  $\tau_d$  expresses the delay time that is supposed to depend on the flow rate. However, as shown in Fig. 4,  $q(\psi)$ 's obtained for several coupling strengths show similar forms; i.e.,  $q(0)$  is almost zero in our case. On the other hand, when the time-delay effect is not negligible, it causes a significant effect on the synchronization phenomena [28,32]. However, even in such a case,  $q(\psi)$  can be obtained in a similar manner simply by estimating  $\tau_d$  and replacing  $\Delta T_i(\psi)$  in Eq. (14) with  $\Delta T_i(\psi + \omega\tau_d)$ .

Next, we will discuss the applicability of the present method to the analysis of multicoupled oscillatory systems. There are several studies on multicoupled BZ oscillators, such as three BZ reactors coupled through mass exchange [8,10] and beads with the catalyst arranged in an array or a lattice structure in the BZ solution [13,15]. The coupling function determined using two coupled oscillators is generally applicable for the analysis of such systems composed of nearly identical oscillators. In this case, it may be possible to deal with the oscillators by using a set of phase equations having an identical coupling function  $q(\psi)$ . As an example, we have performed an analysis for three coupled oscillators by using the obtained  $q(\psi)$ . The phase equations for the three coupled oscillators are given as



$$\frac{d\phi_i}{dt} = \omega_i + \epsilon[q(\phi_i - \phi_j) + q(\phi_i - \phi_k)], \quad (19)$$

where the  $i$ th oscillator is assumed to couple with the other two oscillators designated as  $j$  and  $k$  with  $j \neq k$ . The coupling strength between the oscillators is assumed to be identical. Then, Eq. (19) reduces to the following set of equations:

$$\begin{aligned} \frac{dx}{dt} &= \omega_x + \epsilon[q(x) + q(x+y) - q(y) - q(-x)], \\ \frac{dy}{dt} &= \omega_y + \epsilon[q(y) + q(-x) - q(-x-y) - q(-y)], \end{aligned} \quad (20)$$

where  $x = \phi_1 - \phi_2$ ,  $y = \phi_2 - \phi_3$ ,  $\omega_x = \omega_1 - \omega_2$ , and  $\omega_y = \omega_2 - \omega_3$ . The stationary solutions of Eq. (20) can be obtained graphically by plotting the vector field on a two-dimensional surface. From this analysis, we confirm that several synchronous modes previously reported in the experiment of three coupled oscillators, such as three-phase, partial in-phase, and all in-phase modes [8,13,19], are successfully predicted to appear. The collective behavior of many oscillators can be evaluated by numerical simulation using the obtained  $q(\psi)$ . The detailed description of the application of the present

method to multicoupled oscillators will appear elsewhere.

It is noted that  $q(\psi)$  is also useful for the analysis of unidirectional and asymmetric coupling that was reported previously [8,14]. It is known that the oscillation period tends to be longer under a unidirectional coupling through mass flow. This can be explained in terms of  $q(\psi)$  assuming a negative value when averaged over  $2\pi$ . In asymmetric coupling, where the asymmetry is achieved by employing different volumes of reactors, the analysis can be performed in a manner similar to that in Sec. V by considering the difference in the coupling strength between the two reactors. Thus, the present method shows a potential applicability for any type of coupled-oscillator system whose coupling function is expressed as  $q(\psi)$ . We believe that more complex coupling phenomena in living systems, such as cardiac myocytes [41] and plasmodium [19] on agar microplate, will also be explained in terms of the phase model through the measurement of  $q(\psi)$ .

#### ACKNOWLEDGMENT

This work was partially supported by the Japan Society for the Promotion of Science for Young Scientists.

- 
- [1] A. T. Winfree, *The Geometry of Biological Time* (Springer, New York, 1980).
- [2] A. Pikovsky, M. Rosenblum, and J. Kurths, *Synchronization: A Universal Concept in Nonlinear Sciences* (Cambridge University Press, Cambridge, England, 2001).
- [3] S. C. Manrubia, A. S. Mikhailov, and D. H. Zanette, *Emergence of Dynamical Order: Synchronization Phenomena in Complex Systems* (World Scientific, Singapore, 2004).
- [4] S. Boccaletti, E. Allaria, R. Meucci, and F. T. Arecchi, *Phys. Rev. Lett.* **89**, 194101 (2002).
- [5] J. Buck, *Q. Rev. Biol.* **63**, 265 (1988).
- [6] M. Marek and I. Stuchl, *Biophys. Chem.* **3**, 241 (1975).
- [7] M. F. Crowley and I. R. Epstein, *J. Phys. Chem.* **93**, 2496 (1989).
- [8] M. Yoshimoto, K. Yoshikawa, and Y. Mori, *Phys. Rev. E* **47**, 864 (1993).
- [9] H. Fujii and Y. Sawada, *J. Chem. Phys.* **69**, 3830 (1978).
- [10] K. Nakajima and Y. Sawada, *J. Chem. Phys.* **72**, 2231 (1980).
- [11] K. Bar-Eli, *J. Phys. Chem.* **88**, 3616 (1984).
- [12] M. Boukalouch, J. Elezgaray, A. Arneodo, J. Boissonade, and P. De Kepper, *J. Phys. Chem.* **91**, 5843 (1987).
- [13] N. Nishiyama and K. Eto, *J. Chem. Phys.* **100**, 6977 (1994).
- [14] J. Miyazaki, S. Yoshioka, and S. Kinoshita, *Chem. Phys. Lett.* **387**, 471 (2004).
- [15] H. Fukuda, H. Nagano, and S. Kai, *J. Phys. Soc. Jpn.* **72**, 487 (2003); H. Fukuda, H. Morimura, and S. Kai, *Physica D* **205**, 80 (2005).
- [16] G. Dechert, K.-P. Zeyer, D. Lebender, and F. W. Schneider, *J. Phys. Chem.* **100**, 19043 (1996).
- [17] Y. Kuramoto, *Chemical Oscillation, Wave, and Turbulence* (Springer-Verlag, Berlin, 1984).
- [18] M. Golubitsky, I. Stewart, and D. G. Schaeffer, *Singularities and Groups in Bifurcation Theory*, Vol. II of Applied Mathematical Sciences (Springer, New York, 1988), Vol. 69.
- [19] A. Takamatsu, R. Tanaka, H. Yamada, T. Nakagaki, T. Fujii, and I. Endo, *Phys. Rev. Lett.* **87**, 078102 (2001).
- [20] R. J. Field and R. M. Noyes, *J. Chem. Phys.* **60**, 1877 (1974).
- [21] L. Györgyi and R. J. Field, *Nature (London)* **355**, 808 (1992).
- [22] H. Sakaguchi and Y. Kuramoto, *Prog. Theor. Phys.* **76**, 576 (1986).
- [23] S. H. Strogatz, R. E. Mirollo, and P. C. Matthews, *Phys. Rev. Lett.* **68**, 2730 (1992).
- [24] J. D. Crawford, *J. Stat. Phys.* **74**, 1047 (1994).
- [25] I. Z. Kiss, Y. Zhai, and L. Hudson, *Science* **296**, 1676 (2002).
- [26] H. Daido, *Phys. Rev. Lett.* **73**, 760 (1994); *Int. J. Bifurcation Chaos Appl. Sci. Eng.* **7**, 807 (1997).
- [27] D. Hansel, G. Mato, and C. Meunier, *Phys. Rev. E* **48**, 3470 (1993).
- [28] H. Kori and Y. Kuramoto, *Phys. Rev. E* **63**, 046214 (2001).
- [29] I. Z. Kiss, Y. Zhai, and J. L. Hudson, *Phys. Rev. Lett.* **94**, 248301 (2005).
- [30] J. Miyazaki and S. Kinoshita, *Phys. Rev. Lett.* **96**, 194101 (2006).
- [31] Various definitions of phase such as the Hilbert transformation have been proposed so far, particularly for a chaotic oscillator [2]. However, the phase that is linear with regard to the time development is essential in the present method.
- [32] A. Takamatsu, T. Fujii, and I. Endo, *Phys. Rev. Lett.* **85**, 2026 (2000).
- [33] Z. Zheng, G. Hu, and B. Hu, *Phys. Rev. Lett.* **81**, 5318 (1998).
- [34] W.-H. Kye, D.-S. Lee, S. Rim, C.-M. Kim, and Y.-J. Park, *Phys. Rev. E* **68**, 025201(R) (2003).

- [35] S. Barkin, M. Bixon, R. M. Noyes, and K. Bar-Eli, *Int. J. Chem. Kinet.* **10**, 619 (1978).
- [36] H. D. Försterling, L. Stuk, A. Barr, and W. D. McCormick, *J. Phys. Chem.* **97**, 2623 (1993).
- [37] O. Steinbock, C. T. Hamik, and B. Steinbock, *J. Phys. Chem. A* **104**, 6411 (2000).
- [38] G. Nagy, E. Körös, N. Oftedal, K. Tjelflatt, and R. Ruoff, *Chem. Phys. Lett.* **250**, 255 (1996).
- [39] H. Kitahata, R. Aihara, Y. Mori, and K. Yoshikawa, *J. Phys. Chem. B* **108**, 18956 (2004).
- [40] T. Amemiya, T. Yamamoto, T. Ohmori, and T. Yamaguchi, *J. Phys. Chem. A* **106**, 612 (2002).
- [41] K. Kojima *et al.*, *Lab Chip* **3**, 292 (2003).